Vibrio vulnificus Hemolysin Induces TNF-α Independent ROS Production by Primary Murine Macrophages

Yong-Liang Lou
Xi'an Jiaotong University
Dan-Li Xie
Wenzhou Medical University
Xian-Hui Huang
Wenzhou Medical University
Meng-Meng Zheng
Wenzhou Medical University
Ting Zhang
Jinshan Hospital of Fudan University
Jiru Xu (xujiru@xjtu.edu.cn)
Department of Immunology and Pathogenic Biology, School of Medicine, Xi'an Jiaotong University, Xi'an, Shanxi 710061, China.

Research Article

Keywords: Vibrio vulnificus, hemolysin, ROS, TNF-α

Posted Date: January 22nd, 2021

DOI: https://doi.org/10.21203/rs.3.rs-147505/v1

Abstract

Background

Vibrio vulnificus (V. vulnificus) is a gram-negative opportunistic pathogen that causes lethal infections in humans. *Vibrio vulnificus* hemolysin (VVH) is a key virulence factor that exhibits strong hemolytic and cytolytic activities and contributes to the pathogen's invasion, vasodilatation, and septic shock. Most of the studies so far have focused on VVH's cytolytic activity against cell lines derived from host cells. However, the cytolytic activity of VVH on primary macrophages is still unclear. In addition, although it is known that VVH induces host cell apoptosis via triggering ROS production, the impact of VVH on host immune response has not been fully understood. This study aimed to investigate the role of VVH-induced TNF-α expression and ROS production in the absence of apoptosis of murine primary macrophages and related signaling pathways using FACS, DCFH-DA, real-time PCR, and western blotting.

Results

The results showed that murine primary macrophages from different organs displayed differential sensitivities towards VVH-induced cell death. Liver Kupffer cells, splenic macrophages, and BMMfs were more sensitive to VVH-induced cytotoxicity, while alveolar macrophages, lung interstitial macrophages, and lung neutrophils were resistant to VVH-induced cell death. Besides, we found that a low dose of VVH, which did not induce apoptosis in murine primary macrophages, could induce apoptosis independent TNF-α expression and ROS generation. Such ROS production in macrophages could be further blocked by inhibiting p38-MAPKs or NFκB activation but was not affected by knockout of TNF-α.

Conclusions

VVH produced cytotoxicity in macrophages, an apoptosis-independent TNF-α expression, and ROS production, which provides insight into the mechanism underlying the crosstalk between VVH-induced inflammation and oxidative stress.

Introduction

Vibrio vulnificus (*V. vulnificus*) is a halophilic, gram-negative marine bacterium [1, 2]. As an opportunistic human pathogen that exsits in the envrioment, such as warm sea water. *V. vulnificus* can cause severe life-threatening food poisoning, wound infection, and primary septicemia, especially in patients with hepatitis, hereditary hemochromatosis (HCC), or compromised immune system [3, 4]. Also, *V. vulnificus* infection can cause gastroenteritis, pneumonia, and keratitis. Infections can result from exposing an open wound to contaminated seawater or consuming raw seafood contaminated with *V. vulnificus*, such as oysters. *V. vulnificus* infection's mortality usually exceeds 50%. It can increase to more than 90% in patients who develop sepsis and sepsis-induced organ failure [1]. This hyper-inflammatory response is characterized by massive increases in reactive oxygen species (ROS), nitric oxide (NO), and inflammatory cytokines [5].

V. vulnificus hemolysin (VVH) is a hemolytic and cytotoxic exotoxin that contributes to the invasion of bacteria into the bloodstream [6, 7]. It has been reported that VVH secretion during *V. vulnificus* infection may be involved in increasing vascular permeability, mobilizing P-selectin to the pulmonary endothelial cell surface for adhering to neutrophils, and subsequently causing lung damage [6, 8, 9]. Most of the studies have been focused on the cytotoxic function of VVH, but its immunological functions have not been well elucidated. An early study suggested several clinical strains of *V. vulnificus* induced apoptosis in human and murine macrophage cell lines [10–12]. However, the mechanism and the possibility of *V. vulnificus*-induced death in primary macrophages are unclear. VVH can induce necrosis and apoptosis of multiple cell lineages, such as macrophages and epithelial cells, via different mechanisms [13–15]. It can also induce the continuous production of serum pro-inflammatory cytokines in animals and humans, such as TNF-α and interleukin 10 (IL-10) [16].

ROS plays a significant role in the pathophysiology of bacterial sepsis [17, 18]. Excessive ROS production is harmful to the host cells [19]. However, low ROS levels are also important for cell functioning, particularly for immune cell function against infection [20]. ROS can promote pathogen elimination by direct oxidative damage or by a variety of host defense mechanisms through the immune cells. Immune cells depend on ROS to kill the phagocytosed microorganisms and mediate inflammatory and cellular signaling cascades [21, 22]. Tumor necrosis factor α (TNF-α) is a well-known pro-inflammatory cytokine, important for immunity and cellular homeostasis. Numerous studies have shown that TNF-α and ROS are interconnected, and both play important roles in necrosis and apoptosis. ROS can be induced by cytokines and stimulate pro-inflammatory cytokine production by activating NFκB signaling [23]. Thus, the crosstalk between TNF-α and ROS in inflammation appears complicated and not fully understood. It is known that VVH can induce apoptosis via ROS production in several host cells [13–15, 24, 25]. However, it is unclear whether VVH can induce ROS production and cytokine production in the absence of apoptosis in the innate immune cells. In this study, we investigated the role of VVH-induced TNF-α expression and ROS production in the absence of apoptosis in murine primary macrophages and related signaling pathways.

Materials And Methods

Mice and bacterial strains

C57BL/6 mice were purchased from the Wenzhou Medical University Laboratory Animal Facility. TNF-α$^{-/-}$ mice were generated from the Jackson Laboratory and purchased from the National Animal Resource Information Platform of China. Mice were maintained under an SPF environment at the Central Animal Laboratory of the Wenzhou Medical University. L-929 cells were purchased from the Cell Bank of the Chinese Academy of Science in Shanghai and cultured in RPMI-1640 containing 10% heat-inactivated fetal bovine serum (Ausvin) and penicillin-streptomycin (50 IU/mL and 50 mg/mL; Beyotime). *V. vulnificus* CGMCC 1.1758 strain was provided by the China General Microbiological Culture Collection Center. *V. vulnificus* was cultured at 37°C in the brain heart infusion broth (BHI) or on the BHI rabbit blood

agar plate. *E. coli* BL21 (DE3) was provided by the Key Lab of Laboratory Medicine, Ministry of Education of China. The pMD18T-VvhA plasmid was kindly provided by Dr. Jie Yan (School of Medicine, Zhejiang University, China).

Cloning, expression, purification, and renaturation of VVH

The entire *VvhA* gene was amplified using pMD18T-VvhA as a template by PCR using specific primers (forward, 5'-CCCCATGGTAATGAAAAAAATGACTCTGT-3'; reverse, 3'-TGTAATGTTGTT CAGTTTGAGGAGCTCTT-5'). The PCR product was cloned into the pET28a vector (Novagen, U.S.A.), and the recombinant VVH plasmid was transformed into *E. coli* BL21 (DE3). VVH was expressed in *E.coli* BL21 (DE3) $^{pET28a-VvhA}$ under IPTG induction condition. A small aliquot of the culture was treated with ultrasonic to lysis the cells and extract the protein. After centrifugation, the supernatant and pellet were collected and analyzed for VVH expression by SDS-PAGE and western blotting. As VVH was found in the inclusion body, renaturation of VVH was performed as previously described, with minor modification[26]. Briefly, about one liter of the culture was harvested and sonicated. The inclusion bodies were washed sequentially with solutions 1, 2, and 3 (1, 2 M urea, 10% Triton-X 100, 20 mM Tris-HCl, pH 8.0; 2, 20 mM Tris-HCl pH 8.0; and 3, de-ionized water), and collected after centrifugation at 14,000 g at 4°C. According to the manufacturer's instructions, the inclusion bodies were purified by Ni-NTA affinity chromatography (GE Healthcare Life Science) and assessed by SDS-PAGE. The purified VVH inclusion bodies were denatured by denaturation solution (3 M urea and 20 mM Tris-HCl, pH 8.0) overnight at 4°C. The denatured VVH inclusion bodies were then transferred into dialysis solution 1 (20 mM Tris-HCl, 10.56 mM NaCl, 3 M urea, 100 mM arginine, 5% glycerol, GSH/GSSH, pH 8.5), 2 (20 mM Tris-HCl, 10.56 mM NaCl, 2M urea, 100 mM arginine, 5% glycerol, GSH/GSSH, pH 8.5), 3 (20 mM Tris-HCl, 1M urea, 100 mM arginine, 5% glycerol, pH 8.5), 4 (20 mM Tris-HCl, 100 mM Arginine, 5% Glycerol, pH 8.5), 5 (20 mM Tris-HCl, pH 8.5), and 6 (0.2 M PBS, pH 7.4), sequentially. After dialysis, the refolded VVH in the supernatant was concentrated by vacuum freeze-drying. The specific activity of refolded VVH was 167 hemolytic units/mg (HU/mg), which was confirmed by examining the hemolytic activity against rabbit erythrocytes. The heat-inactivation of VVH was performed by incubating VVH at 65°C for 10 min. One hemolytic unit (HU) level is defined as the amount of VVH present when OD545 RBC suspension (VVH treated)/OD545 RBC suspension = 0.5.

Isolation of total lung single-cell suspension, splenocytes, and liver monocytes

Murine lung was removed from mice with perfusion with 1× PBS (twice), cut into small pieces, incubated in RPMI 1640 containing 20 μg/mL DNase Ⅰ (Beyotime) and 30 μg/mL collagenase Ⅳ (Sigma) for 40 min at 37°C, and passed through a 200 mesh nylon cell filter. Then the cells were washed with RPMI 1640 containing 10% FBS two times. The erythrocytes were lysed with Ammonium-Chloride-Potassium (ACK) lysis buffer. The isolation of liver monocytes and splenocytes was performed as previously described[27].

Generation of bone marrow-derived macrophages (BMMφs)

Bone marrow cells were isolated from femurs and tibiae and then cultured with 10% L-929 cell culture medium (conditioned medium), which was described previously. After 3 days of culture at 37°C in the CO_2 incubator, non-adherent cells were collected and transferred into a new petri dish with a fresh conditioned medium for another 4 d to grow in culture before used for the experiment. The purity of $F4/80^+CD11b^+$ cells was analyzed by flow cytometry. More than 90% of the cells were $F4/80^+CD11b^+$ cells.

Stimulation of cells with VVH in vitro

A total of 1.0×10^6/well total lung cell, splenocytes, or liver monocytes were equally seeded in 48-well plates in a 0.5 mL RPMI-1640 medium containing 10% FBS at various concentrations VVH from 0 to 0.75 HU/mL for 6 h at 37°C in the CO_2 incubator.

For stimulation of BMMφ with VVH, a total of 0.5×10^6/well BMMφ were equally seeded in 48-well plates in 0.5 mL RPMI-1640 medium containing 10% FBS. After overnight incubation at 37°C in the CO_2 incubator, BMMφs were treated with VVH at the indicated concentration and time. For the inhibitor suppression assay, the cells were left without inhibitors (VVH only), with 10 M SB203580 (p38 inhibitor) plus 0.25 HU/mL VVH at 37 ℃ for 6 h, or with 10M BAY11-7082 (NFB inhibitor) plus 0.25 HU/mL at 37 ℃ for 6 h.

Flow cytometry analysis

Flow cytometry analysis was performed as previously described[28]. Cells in single-cell suspension were briefly incubated at 4°C with PBS containing 2% FBS (staining buffer) and fluorescent-conjugated antibodies. After 30 min of incubation, the cells were washed at least two times with staining buffer and resuspended in PBS containing 2% paraformaldehyde. Intracellular staining of cytokines was performed using fixation and permeabilization buffer (eBioscience). All flow cytometry data were collected using the BD FACS Aria (BD Biosciences) and analyzed with the FlowJo software (Treestar).

Measurement of cellular ROS

DCFH-DA (Beyotime) was used to detect cellular ROS production. DCFH-DA became DCF with strong fluorescence once oxidized by cellular ROS. VVH treated cells were loaded with DCFH-DA probes according to the manufacture's protocol. After VVH treatment, cells were briefly incubated with DCFH-DA at 37°C for 30 min in the CO_2 incubator and later stained with other flow antibodies.

Real-time PCR

At each concentration of VVH, RNA was extracted from BMMφs using TRIzol reagent (Invitrogen). cDNA was synthesized using SuperScript III and random primers, and quantitative real time-PCR was performed as described previously. The expression of mRNAs was normalized with β-actin and calculated using the $2^{-\Delta\Delta CT}$ method. Primers used include TNF-α (forward, 5-TGTCTCAGCCTCTTCTCATT-3; reverse, 5-AGATGATCTGAGTGTGAGGG-3).

Western blotting analysis

BMMφs were lysed in RIPA lysis buffer with freshly added protease and phosphatase inhibitor mixtures (Sigma-Aldrich). Lysates from VVH-treated BMMφs were resolved by SDS-PAGE, transferred to a nitrocellulose membrane, and subjected to immunoblotting analysis as described previously. Anti-phospho-p38, anti-phospho-Erk1/2, anti-IKKα/β, and anti-phospho-Akt^{Ser473} were obtained from Cell Signaling Technology. Anti-phospho-NF-κB p65 was procured from Abcam, while anti-β-actin was obtained from Beyotime.

Statistical Analysis

Experimental data are expressed as mean ± SEM. The statistical significance was determined using the two-tailed Student's *t*-test. *, $P < 0.05$; **, $P < 0.01$; ***, $P < 0.001$.

Results

Production and purification of VVH

We first generated prokaryotic VVH expression vector pET28a-VvhA for high-level VVH expression in *E.coli BL21 (DE3)*. The recombinant VVH was expressed in an insoluble form within inclusion bodies (Fig. 1A). High purity VVH was obtained after NTA-Ni^{2+} column affinity purification, reflected in a single protein band having an expected molecular weight of 54 kDa on an SDS-PAGE gel (Fig. 1B). The purified VVH was renatured, and it showed a single band of 54 kDa by Coomassie staining (Fig. 1C) and western blot with an anti-His Tag antibody (Fig. 1D). Refolded VVH demonstrated hemolytic activity against rabbit erythrocytes in a dose-dependent manner (Fig. 1E). After heat inactivation at 65 ℃ for 10 min, VVH lost the hemolytic activity, supporting the assumption that the hemolytic activity was due to VVH.

Analysis of cell death in murine macrophages from various organs under VVH treatment

To investigate the cytotoxicity of VVH towards primary macrophages from different tissues, murine lung single-cell suspension, liver mononuclear cells (MNCs), splenocytes, and bone marrow-derived macrophages (BMMφs) were treated with 0.25, 0.50, or 0.75 HU/mL VVH for 6 h followed by Annexin V or 7-AAD staining to detect cell death. Macrophages of different origins displayed different sensitivities to VVH-induced death. Compared to splenic macrophages, Kupffer cells had a much lower basal death rate but displayed a much higher death rate following VVH treatment (Fig. 2A and 2B). Previous studies showed that VVH could induce murine lung vascular structures' dysfunction by increasing vascular permeability and neutrophil sequestration [29]. Although a majority of the alveolar Mφ (AM) and interstitial Mφ (IM) died during in vitro culture without VVH treatment, VVH treatment did not induce additional cell death. Moreover, VVH did not display obvious cytotoxicity to neutrophils (Fig. 2C and 2D).

Low dose VVH triggers reactive oxygen species production without triggering cell death

Similar to the liver and splenic myeloid cells, $CD11b^{+}F4/80^{+}$ BMMφs were sensitive to high dose (> 0.25 HU/mL) VVH induced death, but cells were resistant to low dose (0.25 HU/mL) VVH treatment (Fig. 3A and 3B). As a low dose is more relevant to the early phase of infection, we sought to investigate BMMφs response to treatment with a low dose of VVH. As ROS production is associated with VVH-induced cell death, we first investigated whether low dose VVH treatment induces ROS production activity. To our surprise, we detected elevated ROS levels in BMMφs treated with 0.25 HU/mL VVH using DCF staining and flow cytometry (Fig. 3C). Besides, in contrast to activated VVH, the heat-inactivated VVH treatment also showed the ROS production was slightly increased, indicating that VVH cytotoxicity's independence was probably involved in VVH-triggered ROS production.

To investigate how VVH induces ROS production in BMMφs, we examined MAPK and NFκB signaling pathways, two important pathways for ROS production. As shown in (Fig. 3D), 0.25 HU/mL VVH treatment-induced IKKβ, NFκB, and p38-MAPK, but not ERK1/2 or AKT phosphorylation in BMMφs. Moreover, inhibition of p38 with a chemical inhibitor SB203580 abolished VVH-induced ROS production, while NFκB inhibitor BAY 11-7082 partially inhibited VVH-induced ROS production (Fig. 3E). These data suggest that low dose VVH can induce cellular oxidative stress by inducing ROS production through activation of p38-MAPK and NFκB pathways.

Low dose VVH induces pro-inflammatory cytokine production in murine BMMφs

To investigate whether low dose VVH treatment can induce pro-inflammatory cytokine production, we focused on TNF-α. We observed that 0.25 HU/mL VVH did not cause the death of primary murine BMMφs, but induction of TNF-α production did, which was detected by intracellular staining. The frequency of $TNF\text{-}\alpha^{+}$ BMMφs was 18.8% in the 0.25 HU/mL VVH treatment group, 5.64% in the inactivated 0.25 HU/mL VVH treatment group, and 1.3% in the PBS control (Fig. 4A and 4B). Consistent with the flow cytometry data, the TNF-α mRNA expression was also upregulated in murine BMMφs (Fig. 4C). These data indicate that low dose VVH can promote TNF-α production via inducing TNF-α transcription, which may trigger inflammatory responses at a very early stage of *V. vulnificus* infection.

ROS generation independent of TNF-α in BMMφs upon VVH treatment

Our data show that low dose VVH induces TNF-α production and ROS generation in BMMφs. As TNF-α has been reported to induce ROS production in macrophages [30], VVH-induced ROS generation could be indirectly caused by TNF-α. To determine the role of TNF-α in VVH-induced ROS production, we treated WT and $TNF\alpha^{-/-}$ BMMφs with 0.25 HU/mL VVH. $TNF\alpha^{-/-}$ mice did not produce TNFα (Fig. 5A). $TNF\alpha^{-/-}$ BMMφs produced ROS levels similar to WT controls (Fig. 5B). These data indicate that VVH induces ROS independent of TNF-α.

Discussion

It has been reported that several clinical strains of *V. vulnificus* induce apoptosis in human and murine macrophage cell lines [10, 31]. In this study, we showed that VVH could induce the death of murine primary macrophages. We further showed that murine macrophages from different organs display differential sensitivities to VVH-induced cell death. Liver Kupffer cells, splenic macrophages, and BMMφs are more sensitive to the cytotoxicity of VVH, while alveolar macrophages, lung interstitial macrophages, and lung neutrophils are resistant to VVH-induced cell death. The mechanisms that dictate the sensitivities of these cells towards VVH are unclear. One possibility is that VVH may partially inhibit innate immune responses in the spleen and liver by inducing macrophage death in these organs at an early stage of *V. vulnificus* infection.

To its hemolytic and cytolytic activities, the effects of VVH on immune cells have not been well defined. Previous studies have shown that pathogens' hemolysin could affect the host cells by triggering various cellular events, such as cell death or ROS production. *Streptolysin* O (SLO) triggers cell death through apoptosis in macrophages and neutrophils [32], and SLO also activates p38 via ASK1 and ROS [33]. Like SLO, *Listeriolysin* O(LLO)also triggers apoptosis in dendritic cells and T lymphocytes [34]. Moreover, nitric oxide (NO) production depends on high doses of pneumolysin (PLY) treatment and phagocytosis. However, the low dose of PLY mainly induces rapid ROS production [35]. Other hemolysins, such as hemolysin II (HlyII) of *Bacillus cereus*, have also been reported could induce apoptosis in host monocytes and macrophages in vivo [36]. During phagocytosis, the phagocytes internalized the microbes, such as *L. interrogans* that produce rSph2 hemolysin, which could directly target the mitochondria, and trigger cell apoptosis by induction of ROS and mitochondrial membrane damage [37]. This study found that the low dose of VVH could induce significant ROS production even without triggering apoptosis. To date, only the high dose of VVH has been reported to induce ROS production in epithelial cells and endothelial cells upon apoptosis [14, 15, 24, 38, 39]. The high dose of VVH induced cell death and ROS production through phosphorylation of a distinct ERK1/2 kinase [15, 25], and ERK1/2 did not respond to treatment with the low dose of VVH in murine BMMφs. We found that the low dose of VVH treatment elevated phosphorylation of p38, Akt, NFκB, and IKKα/β in murine BMMφs, and that low dose VVH triggered both p38-MAPKs- and NFκB-dependent ROS generation. Thus, the mechanisms of ROS production are likely different between low dose of VVH and high dose of VVH treatment.

TNF-α and IL-1 are two important mediators leading to sepsis. Previous studies have reported that VVH can induce the release of IL-1β, but not TNF-α in macrophages [40]. In this study, we found that a low dose of VVH can directly induce TNF-α expression. Our result is in line with a previous observation that VVH treatment increases TNF-α and IL-10 levels in murine serum [16]. For other pathogens, previous reports show that *Leptospiral* hemolysin induces TNF-α, IL-1β, and IL-6 levels in murine macrophages via toll-like receptor 2 (TLR2)- or TLR4-mediated JNK and NFκB pathways [41]. Sub-cytocidal concentrations of α-hemolysin from *E. coli* could lead to increased IL-1β production, but not that of TNF-α in monocytes [42]. Another hemolysin study reported that it was associated with triggering inflammation. SLO inhibited TNF-α and IL-1β release from infected macrophages to blunt macrophages' immune response [32]. LLO causes IL-1β production by activating NLRP3 inflammasome in macrophages [43] and inducing cytokine gene expression, including IL-1, TNF-α, IFN-γ, and IL-12 [44]. However, the expression of IL-1β, IL-6, and IL-

8 was not affected by PLY. Only the TNF-α level was enhanced by PLY in a phagocytosis-independent manner [35]. *Vibrio parahaemolyticus* plays a major role in triggering NLRP3 inflammasome activation with IL-1β secretion in macrophages [45]. Thus, inflammation cytokines production by VVH appears to be different from that of other hemolysins.

The results of this study also provide additional insights into the relationship between TNF-α and ROS. Both TNF-α and ROS are crucial for inflammation, but the crosstalk between ROS and TNF-α during Infection is still not fully understood. The lectin-like domain of TNF-α has been reported to decrease LLO-induced *Nox4* mRNA expression and ROS generation [46]. TNF-α activates NFκB signaling pathway in apoptotic cells and subsequently inhibits intracellular ROS level [23]. However, ROS generation is also induced by cytokines. In phagocytes, activation of the TNF-NOX2 signaling leads to ROS production responsible for inflammation and associated tissue damage [47]. Pore-forming toxin from *Serratia marcescens* can cause TNF-α-dependent necroptosis and facilitate ROS generation [48]. Thus, TNF is also important for ROS production. In this study, we showed that knockout TNF-α in murine macrophages does not affect ROS generation by low dose VVH treatment, which differs from the classic interconnection between TNF and ROS. Future work will focus on the mechanism underlying VVH-induced inflammation and oxidation stress.

Declarations

ETHICS APPROVAL AND CONSENT TO PARTICIPATE

All animal experiments were performed according to the guidelines of the Zhejiang Provincial Animal Care and Use Administration Office (SYXK-ZJ-2005-0061) and the protocols approved by the Wenzhou Medical University Animal Care and Use Committee (reference: wydw2014-0009).

CONSENT FOR PUBLICATION

Not applicable.

AVAILABILITY OF DATA AND MATERIALS

The datasets used and/or analyzed during the current study are available from the corresponding author on reasonable request.

COMPETING INTERESTS

All the authors declare there are no competing interests.

FUNDING

The study was supported by Wenzhou Science and Technology Funds (Y20150113 to D.L.X.), Zhejiang Provincial Natural Science Foundation Grant (LY13H190007 to D.L.X.), and Chinese National Natural Science Foundation Grant (31400763 to D.L.X.).

AUTHORS' CONTRIBUTIONS

Y. L., D.X., and J.X. conceived and designed experiments. Y. L., D.X., X.H., M. Z., T. Z., and J.X. analyzed the data, conducted the experiments. Y. L., D.X., and J.X. wrote the manuscript.

ACKNOWLEDGMENTS

We thank the Flow Cytometry Core Facility of the China Ministry of Education Key Lab of Laboratory Medicine at the Wenzhou Medical University for their services.

AUTHORS'S STATEMENTS

We confirm that all methods were carried out in accordance with relevant guidelines and regulations. We also confirm that the study was carried out in compliance with the ARRIVE guidelines.

References

1. Lee YC, Hor LI, Chiu HY, Lee JW, Shieh SJ. Prognostic factor of mortality and its clinical implications in patients with necrotizing fasciitis caused by Vibrio vulnificus. European journal of clinical microbiology & infectious diseases : official publication of the European Society of Clinical Microbiology. 2014;33(6):1011-8; doi: 10.1007/s10096-013-2039-x.
2. Park J, Lee CS. Vibrio vulnificus Infection. N Engl J Med. 2018;379(4):375; doi: 10.1056/NEJMicm1716464.
3. Ryu HH, Lee JY, Yun NR, Kim DM. Necrotizing soft tissue infection with gas formation caused by Vibrio vulnificus and misdiagnosed as Pseudomonas aeruginosa. The American journal of emergency medicine. 2013;31(2):464 e5-8; doi: 10.1016/j.ajem.2012.09.001.
4. Baker-Austin C, Oliver JD. Vibrio vulnificus: new insights into a deadly opportunistic pathogen. Environ Microbiol. 2018;20(2):423-30; doi: 10.1111/1462-2920.13955.
5. Victor VM, Espulgues JV, Hernandez-Mijares A, Rocha M. Oxidative stress and mitochondrial dysfunction in sepsis: a potential therapy with mitochondria-targeted antioxidants. Infectious disorders drug targets. 2009;9(4):376-89.
6. Lee SE, Ryu PY, Kim SY, Kim YR, Koh JT, Kim OJ, et al. Production of Vibrio vulnificus hemolysin in vivo and its pathogenic significance. Biochemical and biophysical research communications. 2004;324(1):86-91; doi: 10.1016/j.bbrc.2004.09.020.
7. Wright AC, Morris JG, Jr., Maneval DR, Jr., Richardson K, Kaper JB. Cloning of the cytotoxin-hemolysin gene of Vibrio vulnificus. Infection and immunity. 1985;50(3):922-4.
8. Lee YR, Park KH, Lin ZZ, Kho YJ, Park JW, Rho HW, et al. A calcium-calmodulin antagonist blocks experimental Vibrio vulnificus cytolysin-induced lethality in an experimental mouse model. Infection and immunity. 2004;72(10):6157-9; doi: 10.1128/IAI.72.10.6157-6159.2004.

9. Park JW, Ma SN, Song ES, Song CH, Chae MR, Park BH, et al. Pulmonary damage by Vibrio vulnificus cytolysin. Infection and immunity. 1996;64(7):2873-6.
10. Kashimoto T, Ueno S, Hanajima M, Hayashi H, Akeda Y, Miyoshi S, et al. Vibrio vulnificus induces macrophage apoptosis in vitro and in vivo. Infect Immun. 2003;71(1):533-5; doi: 10.1128/iai.71.1.533-535.2003.
11. Shin NR, Lee DY, Shin SJ, Kim KS, Yoo HS. Regulation of proinflammatory mediator production in RAW264.7 macrophage by Vibrio vulnificus luxS and smcR. FEMS Immunol Med Microbiol. 2004;41(2):169-76; doi: 10.1016/j.femsim.2004.03.001.
12. Murciano C, Hor LI, Amaro C. Host-pathogen interactions in Vibrio vulnificus: responses of monocytes and vascular endothelial cells to live bacteria. Future microbiology. 2015;10(4):471-87; doi: 10.2217/fmb.14.136.
13. Jeong HG, Satchell KJ. Additive function of Vibrio vulnificus MARTX(Vv) and VvhA cytolysins promotes rapid growth and epithelial tissue necrosis during intestinal infection. PLoS Pathog. 2012;8(3):e1002581; doi: 10.1371/journal.ppat.1002581.
14. Lee SJ, Lee HJ, Jung YH, Kim JS, Choi SH, Han HJ. Melatonin inhibits apoptotic cell death induced by Vibrio vulnificus VvhA via melatonin receptor 2 coupling with NCF-1. Cell death & disease. 2018;9(2):48; doi: 10.1038/s41419-017-0083-7.
15. Lee SJ, Jung YH, Oh SY, Song EJ, Choi SH, Han HJ. Vibrio vulnificus VvhA induces NF-kappaB-dependent mitochondrial cell death via lipid raft-mediated ROS production in intestinal epithelial cells. Cell death & disease. 2015;6:1655; doi: 10.1038/cddis.2015.19.
16. Chun JH CS, Park SD. Significance of Blood TNF-alpha and Interleukin 10 Levels in Vibrio Vulnificus Cytolysin Toxemia. Korean Journal of Dermatology. 2001;39(6):5.
17. Marschall R, Tudzynski P. Reactive oxygen species in development and infection processes. Seminars in cell & developmental biology. 2016;57:138-46; doi: 10.1016/j.semcdb.2016.03.020.
18. Spooner R, Yilmaz O. The role of reactive-oxygen-species in microbial persistence and inflammation. International journal of molecular sciences. 2011;12(1):334-52; doi: 10.3390/ijms12010334.
19. Di Meo S, Reed TT, Venditti P, Victor VM. Harmful and Beneficial Role of ROS. Oxidative medicine and cellular longevity. 2016;2016:7909186; doi: 10.1155/2016/7909186.
20. West AP, Brodsky IE, Rahner C, Woo DK, Erdjument-Bromage H, Tempst P, et al. TLR signalling augments macrophage bactericidal activity through mitochondrial ROS. Nature. 2011;472(7344):476-80; doi: 10.1038/nature09973.
21. Gery I, O'Brien PJ. RCS rat macrophages exhibit normal ROS phagocytosis. Investigative ophthalmology & visual science. 1981;20(5):675-9.
22. Zhu S, Wang Y, Wang X, Li J, Hu F. Emodin inhibits ATP-induced IL-1beta secretion, ROS production and phagocytosis attenuation in rat peritoneal macrophages via antagonizing P2X(7) receptor. Pharmaceutical biology. 2014;52(1):51-7; doi: 10.3109/13880209.2013.810648.
23. Blaser H, Dostert C, Mak TW, Brenner D. TNF and ROS Crosstalk in Inflammation. Trends in cell biology. 2016;26(4):249-61; doi: 10.1016/j.tcb.2015.12.002.

24. Kwon KB, Yang JY, Ryu DG, Rho HW, Kim JS, Park JW, et al. Vibrio vulnificus cytolysin induces superoxide anion-initiated apoptotic signaling pathway in human ECV304 cells. The Journal of biological chemistry. 2001;276(50):47518-23; doi: 10.1074/jbc.M108645200.
25. Song EJ, Lee SJ, Lim HS, Kim JS, Jang KK, Choi SH, et al. Vibrio vulnificus VvhA induces autophagy-related cell death through the lipid raft-dependent c-Src/NOX signaling pathway. Scientific reports. 2016;6:27080; doi: 10.1038/srep27080.
26. Long S, Truong L, Bennett K, Phillips A, Wong-Staal F, Ma H. Expression, purification, and renaturation of bone morphogenetic protein-2 from Escherichia coli. 46(2):0-378.
27. Wu J, Shin J, Xie D, Wang H, Gao J, Zhong XP. Tuberous sclerosis 1 promotes invariant NKT cell anergy and inhibits invariant NKT cell-mediated antitumor immunity. J Immunol. 2014;192(6):2643-50; doi: 10.4049/jimmunol.1302076.
28. Xie DL, Zheng MM, Zheng Y, Gao H, Zhang J, Zhang T, et al. Vibrio vulnificus induces mTOR activation and inflammatory responses in macrophages. PLoS One. 2017;12(7):e0181454; doi: 10.1371/journal.pone.0181454.
29. Ooe K. Pulmonary damage by Vibrio vulnificus cytolysin. Infection and immunity. 1997;65(4):1570.
30. Roca FJ, Ramakrishnan L. TNF dually mediates resistance and susceptibility to mycobacteria via mitochondrial reactive oxygen species. Cell. 2013;153(3):521-34; doi: 10.1016/j.cell.2013.03.022.
31. Tsuchiya T, Mitsuo E, Hayashi N, Hikita Y, Nakao H, Yamamoto S, et al. Vibrio vulnificus damages macrophages during the early phase of infection. Infection and immunity. 2007;75(9):4592-6; doi: 10.1128/IAI.00481-07.
32. Timmer AM, Timmer JC, Pence MA, Hsu L-C, Ghochani M, Frey TG, et al. Streptolysin O promotes group A Streptococcus immune evasion by accelerated macrophage apoptosis. The Journal of biological chemistry. 2009;284(2):862-71; doi: 10.1074/jbc.M804632200.
33. Husmann M, Dersch K, Bobkiewicz W, Beckmann E, Veerachato G, Bhakdi S. Differential role of p38 mitogen activated protein kinase for cellular recovery from attack by pore-forming S. aureus alpha-toxin or streptolysin O. Biochem Biophys Res Commun. 2006;344(4):1128-34; doi: 10.1016/j.bbrc.2006.03.241.
34. Carrero JA, Calderon B, Vivanco-Cid H, Unanue ER. Recombinant Listeria monocytogenes expressing a cell wall-associated listeriolysin O is weakly virulent but immunogenic. Infect Immun. 2009;77(10):4371-82; doi: 10.1128/iai.00419-09.
35. Martner A, Dahlgren C, Paton JC, Wold AE. Pneumolysin released during Streptococcus pneumoniae autolysis is a potent activator of intracellular oxygen radical production in neutrophils. Infect Immun. 2008;76(9):4079-87; doi: 10.1128/iai.01747-07.
36. Tran SL, Guillemet E, Ngo-Camus M, Clybouw C, Puhar A, Moris A, et al. Haemolysin II is a Bacillus cereus virulence factor that induces apoptosis of macrophages. Cellular microbiology. 2011;13(1):92-108; doi: 10.1111/j.1462-5822.2010.01522.x.
37. Che R, Ding S, Zhang Q, Yang W, Yan J, Lin X. Haemolysin Sph2 of Leptospira interrogans induces cell apoptosis via intracellular reactive oxygen species elevation and mitochondrial membrane injury.

Cellular microbiology. 2019;21(1):e12959; doi: 10.1111/cmi.12959.

38. Kim BS, Kim JS. Vibrio vulnificus cytolysin induces hyperadhesiveness of pulmonary endothelial cells for neutrophils through endothelial P-selectin: a mechanism for pulmonary damage by Vibrio vulnificus cytolysin. Experimental & molecular medicine. 2002;34(4):308-12; doi: 10.1038/emm.2002.43.
39. Rho HW, Choi MJ, Lee JN, Park JW, Kim JS, Park BH, et al. Cytotoxic mechanism of Vibrio vulnificus cytolysin in CPAE cells. Life sciences. 2002;70(16):1923-34.
40. Toma C, Higa N, Koizumi Y, Nakasone N, Ogura Y, McCoy AJ, et al. Pathogenic Vibrio activate NLRP3 inflammasome via cytotoxins and TLR/nucleotide-binding oligomerization domain-mediated NF-kappa B signaling. J Immunol. 2010;184(9):5287-97; doi: 10.4049/jimmunol.0903536.
41. Wang H, Wu Y, Ojcius DM, Yang XF, Zhang C, Ding S, et al. Leptospiral hemolysins induce proinflammatory cytokines through Toll-like receptor 2-and 4-mediated JNK and NF-kappaB signaling pathways. PloS one. 2012;7(8):e42266; doi: 10.1371/journal.pone.0042266.
42. Bhakdi S, Muhly M, Korom S, Schmidt G. Effects of Escherichia coli hemolysin on human monocytes. Cytocidal action and stimulation of interleukin 1 release. The Journal of clinical investigation. 1990;85(6):1746-53; doi: 10.1172/JCI114631.
43. Tsukada H, Kawamura I, Fujimura T, Igarashi K, Arakawa M, Mitsuyama M. Induction of macrophage interleukin-1 production by Listeria monocytogenes hemolysin. Cellular immunology. 1992;140(1):21-30; doi: 10.1016/0008-8749(92)90173-m.
44. Nishibori T, Xiong H, Kawamura I, Arakawa M, Mitsuyama M. Induction of cytokine gene expression by listeriolysin O and roles of macrophages and NK cells. Infect Immun. 1996;64(8):3188-95.
45. Higa N, Toma C, Koizumi Y, Nakasone N, Nohara T, Masumoto J, et al. Vibrio parahaemolyticus effector proteins suppress inflammasome activation by interfering with host autophagy signaling. PLoS Pathog. 2013;9(1):e1003142; doi: 10.1371/journal.ppat.1003142.
46. Xiong C, Yang G, Kumar S, Aggarwal S, Leustik M, Snead C, et al. The lectin-like domain of TNF protects from listeriolysin-induced hyperpermeability in human pulmonary microvascular endothelial cells - a crucial role for protein kinase C-alpha inhibition. Vascular pharmacology. 2010;52(5-6):207-13; doi: 10.1016/j.vph.2009.12.010.
47. Forman HJ, Torres M. Reactive oxygen species and cell signaling: respiratory burst in macrophage signaling. American journal of respiratory and critical care medicine. 2002;166(12 Pt 2):S4-8; doi: 10.1164/rccm.2206007.
48. Gonzalez-Juarbe N, Gilley RP, Hinojosa CA, Bradley KM, Kamei A, Gao G, et al. Pore-Forming Toxins Induce Macrophage Necroptosis during Acute Bacterial Pneumonia. PLoS pathogens. 2015;11(12):e1005337; doi: 10.1371/journal.ppat.1005337.

Figures

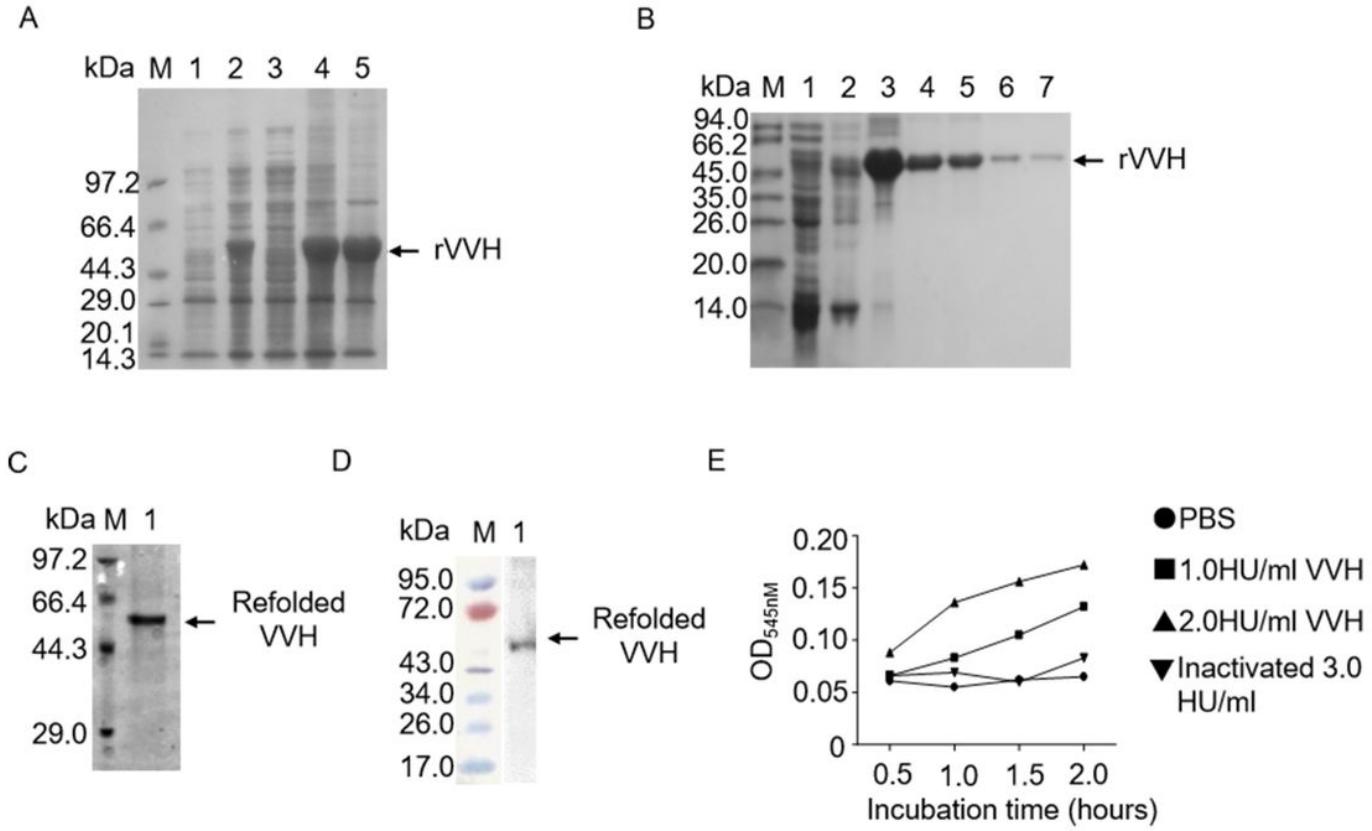

Figure 1

Hemolytic activity of recombinant VVH on rabbit erythrocytes. (A) Expression of recombinant VVH. Lysates or supernatants of the E. coli BL21 DE3 pET28a-VvhA culture after overnight culture with or without IPTG induction were subjected to SDS-PAGE followed by Coomassie blue staining. M, molecular weight marker; 1, whole lysate without IPTG induction; 2, whole lysate after 0.5 mM IPTG induction; 3, the supernatant of culture after 0.5 mM IPTG induction; 4, duplicate lane 2, and add with more bacteria. 5, Purified inclusion bodies. (B) Assessment of VVH purification. VVH in inclusion body preparation was purified by NTA-Ni2+ affinity chromatography column. M, molecular weight marker; 1, flow-through elution; 2, NTA-0 elution (0 mM imidazole); 3, NTA-20 elution (20 mM imidazole); 4, NTA-60 elution (60 mM imidazole); 5, NTA-100 elution (100 mM imidazole); 6, NTA-1000 elution (1000 mM imidazole). (C-D) The identification of refolded VVH was performed by SDS-PAGE (C), and western blot (D). Lanes: M, molecular weight marker; 1, purified refolded-VVH. (E) The hemolytic activity of VVH against rabbit erythrocytes.

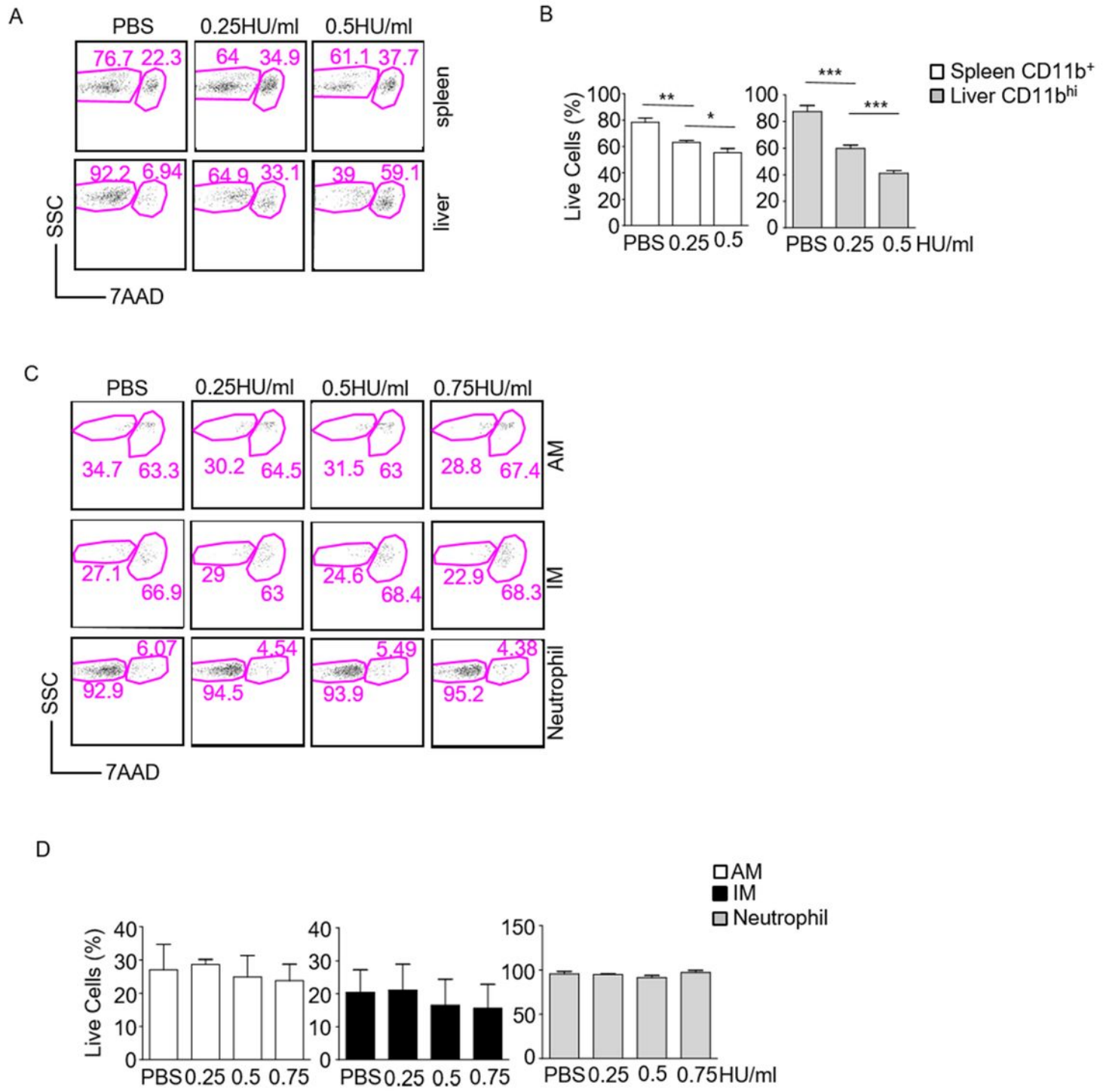

Figure 2

Differences in VVH cytotoxicity to murine primary macrophages in various tissues. Single-cell suspension from the lung, spleen, and liver MNCs were treated with PBS or VVH in vitro at 37 ℃ for 6 h. The cells were stained for CD11b, F4/80, and 7-AAD and analyzed by FACS. (A, C) Dot plots showed 7-AAD staining of gated CD11b+F4/80+ (spleen), CD11bhi F4/80+ (liver) cells, CD45.2+CD68hiF4/80hiCD11b-CD11chiIA-IElow (lung alveolar macrophage, AM), CD45.2+CD68lowF4/80lowCD11b+Gr1-CD11clow

(lung interstitial macrophage, IM) or CD45.2+CD68-F4/80-CD11b+Gr1hi (lung neutrophil). (B, D) Bar graphs with mean ± SEM of live cells. Data shown are representative of at least three experiments. Data shown are representative of at least three experiments. *, P<0.05; **, P<0.01; ***, P<0.001 determined by the Student's t-test.

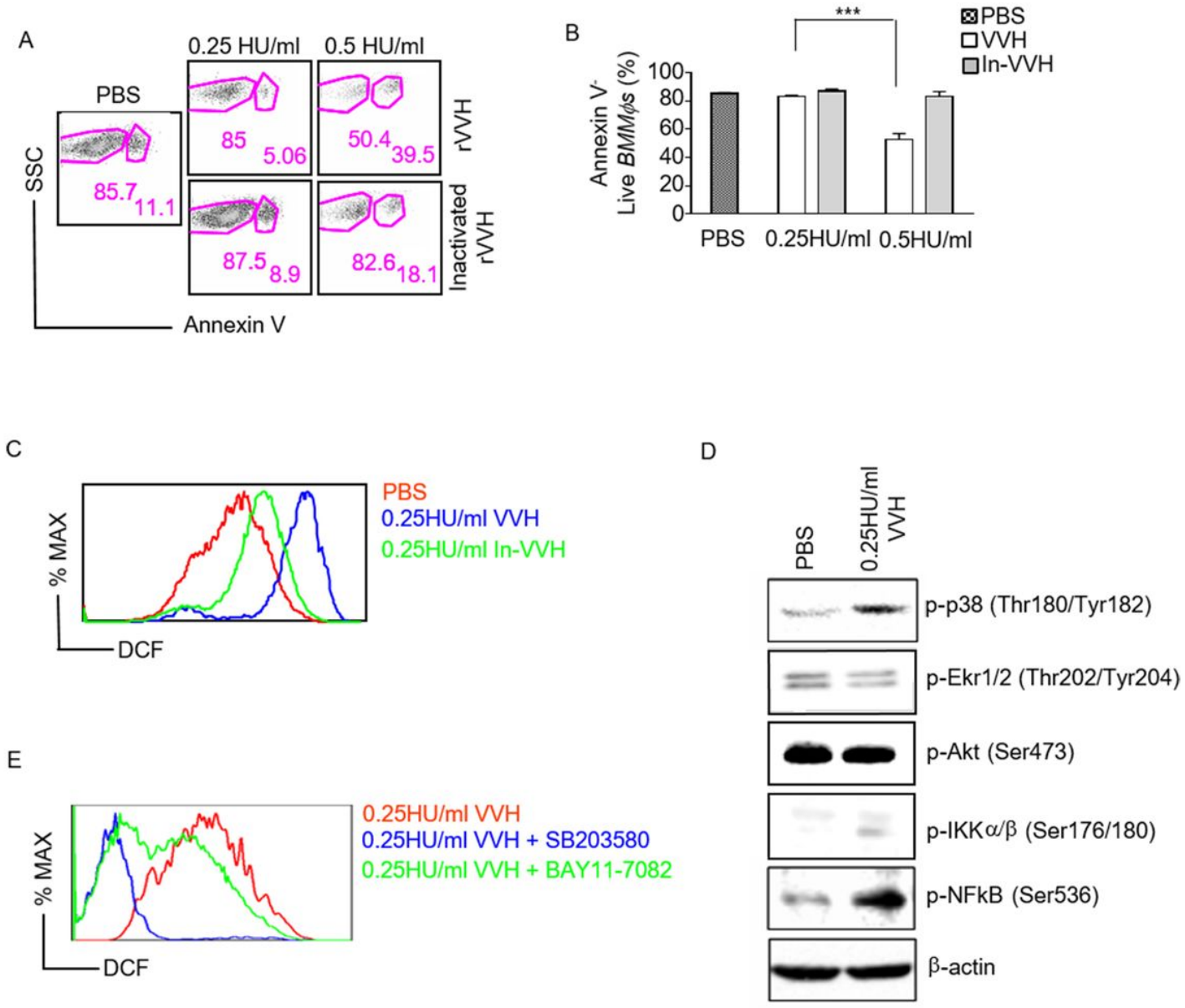

Figure 3

Low dose VVH induces ROS generation in the absence of apoptosis. (A, B) Elevated cell death in BMMØs after VVH treatment in vitro. Representative dot plots of Annexin-V staining in gated CD11b+F4/80+ murine BMMØs are shown. (C) Increased ROS production in BMMØs after VVH stimulation in vitro. Overlaid histogram shows DCF intensity in live-gated CD11b+BMMØs. (D) VVH induces p38-MAPK and NFØB activation in BMMØs. Cell lysates from murine BMMØs treated with or without 0.25 HU/mL VVH

stimulation for 6 h were subjected to western blot analysis with the indicated antibodies. (E) Inhibition of ROS generation in VVH treated BMMØs by 10 μM p38 inhibitor SB203580, or 10 μM NFØB inhibitor BAY11-7082. Overlaid histogram shows DCF intensity in live-gated BMMØs. Data shown are representative of three experiments.

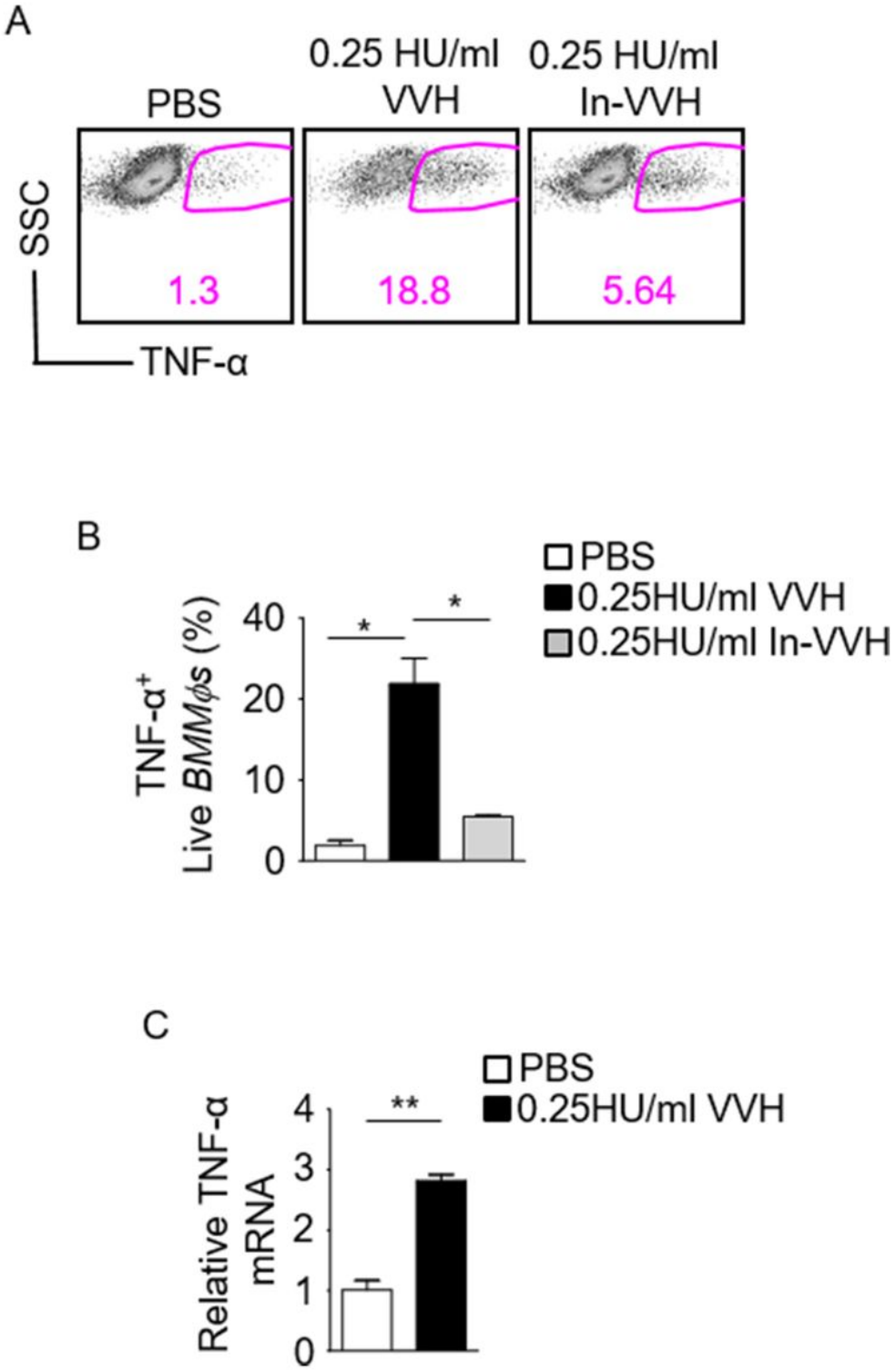

Figure 4

Low dose VVH induces TNF-α production in the absence of apoptosis. (A, B) BMMØs were stimulated with VVH in the presence of 1 ng/mL GolgiPlug for 6 h in vitro. Dot plots show TNF-α expression in live-gated CD11b+F4/80+ BMMØs. (C) Increased TNF-α expression and elevated TNF-α mRNA levels in murine BMMØs following VVH stimulation in vitro. Bar graphs with mean ± SEM of live cells. Data shown are representative of at least three experiments. In-VVH stands for heat-inactivated VVH. *, P<0.05; **, P<0.01; ***, P<0.001 as determined by two-tailed Student t-test.

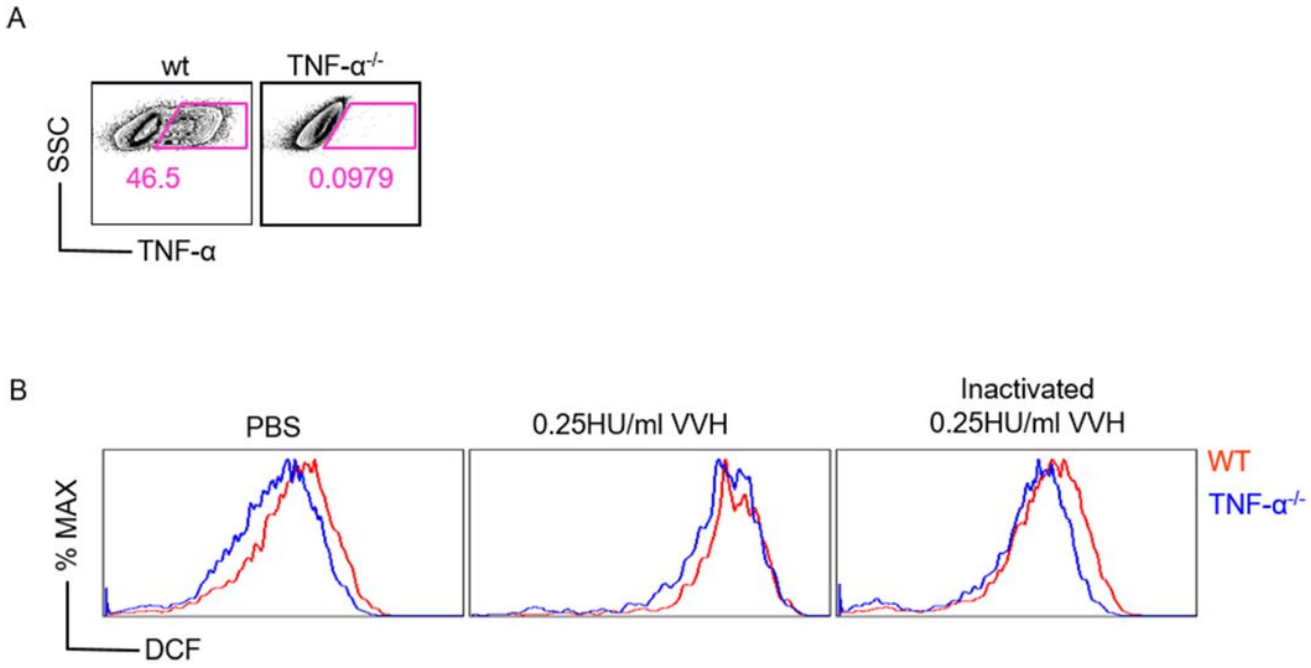

Figure 5

VVH-induced ROS production is independent of TNF-α (A) Absence of TNF-α in TNF-α deficient murine BMMØs following 5 ng/mL LPS stimulation presence of 1 ng/mL GolgiPlug for 4 h in vitro. FACS plots show intracellular TNF-α staining in live-gated CD11b+ BMMØs. (B) TNF-α is not essential for VVH-induced ROS generation in BMMØs. WT and TNFα deficient BMMØs were similarly stimulated, and examined as above in Figure 4C. Data shown are representative of at least three experiments.